International Journal of Minerals, Metallurgy and Materials
Volume 27, Number 1, January 2020, Page 100
https://doi.org/10.1007/s12613-019-1909-3

Influence of carbon-partitioning treatment on the microstructure, mechanical properties and wear resistance of *in situ* VCp-reinforced Fe-matrix composite

Ping-hu Chen[1)], *Yun Zhang*[2)], *Rui-qing Li*[2)], *Yan-xing Liu*[3)], *and Song-sheng Zeng*[4)]

1) School of Advanced Materials, Peking University Shenzhen Graduate School, Shenzhen 518055, China
2) Light Alloy Research Institutes and State Key Laboratory of High Performance Complex Manufacturing, Central South University, Changsha 410083, China
3) School of Mechanical Engineering, DongGuan University of Technology, Dongguan 523808, China
4) Valin ArcelorMittal Automotive Steel Co., Ltd., Loudi 417000, China
(Received: 31 May 2019; revised: 25 September 2019; accepted: 27 September 2019)

Abstract: The wear resistance of iron (Fe)-matrix materials could be improved through the *in situ* formation of vanadium carbide particles (VCp) with high hardness. However, brittleness and low impact toughness limit their application in several industries due to addition of higher carbon content. Carbon-partitioning treatment plays an important role in tuning the microstructure and mechanical properties of *in situ* VCp-reinforced Fe-matrix composite. In this study, the influences of carbon-partitioning temperatures and times on the microstructure, mechanical properties, and wear resistance of *in situ* VCp-reinforced Fe-matrix composite were investigated. The experimental results indicated that a certain amount of retained austenite could be stabilized at room temperature through the carbon-partitioning treatment. Microhardness of *in situ* VCp-reinforced Fe-matrix composite under carbon-partitioning treatment could be decreased, but impact toughness was improved accordingly when wear resistance was enhanced. In addition, the enhancement of wear resistance could be attributed to transformation-induced plasticity (TRIP) effect, and phase transformation was caused from γ-Fe (face-centered cubic structure, fcc) to α-Fe (body-centered cubic structure, bcc) under a certain load.

Keywords: carbon-partitioning treatment; retained austenite; phase transformation; mechanical properties; wear resistance

1. Introduction

Vanadium is a strong carbide-forming element [1−2], which is widely used to prepare *in situ* vanadium carbide particle (VCp)-reinforced iron (Fe)-matrix composites (VCFC) [3−4]. The VCFC exhibits a combination of the excellent mechanical properties of the matrix and the high hardness of vanadium carbide (VC) [5−7], i.e., HV 2800 [8], which is higher than that of Cr_7C_3 (HV 1300–1500) [9]. Therefore, the VCFC has been widely used for wear-resistant components that are subjected to considerable wear and impact [10−11]. Wei and colleagues [12−13] investigated the influence of VC (*in situ* synthetized with vanadium and carbon) on the wear resistance of high-vanadium high-speed steel (HVHSS). Their results indicated that the wear resistance of HVHSS is three times that of high-chromium cast iron and eight times that of high manganese steel [12]. However, many engineering applications are seriously restricted by the high manufacturing cost because of the long period of heat treatment at high temperature [14]. In addition, serious degeneration of the mechanical properties was caused by the high-temperature oxidation and volatilization of V-rich and Mo-rich oxides [15]. In our previous works, high-temperature oxidation resistance was investigated under the conditions of different manganese contents and oxidation temperatures [16−17], and the alloying elements were adjusted to improve the high-temperature oxidation resistance and decrease the manufacturing cost. However, two major issues, namely, poor toughness and serious brittleness, were caused by the high carbon content. Therefore, a new *in situ* VCFC with excellent comprehensive performance is designed on the basis of the transformation-induced plasticity (TRIP) effect [18−19] and quenching and partitioning (Q&P) heat treatment [20−21].

Corresponding authors: Rui-qing Li E-mail: liruiqing@csu.edu.cn; Song-sheng Zeng E-mail: zsscsu@sina.com

TRIP steel was designed and developed in the middle of the last century [22]. Previous research showed that metastable austenite is transformed into martensite under a certain additional load, thus improving the mechanical properties [23−24]. Subsequently, Speer and colleagues [25−26] discovered that retained austenite can be stabilized at room temperature through Q&P heat treatment and phase transformation from retained austenite to martensite occurred under a certain load (regarded as the TRIP effect), thus resulting in extensive applications of the materials. A previous study [27] reported that retained austenite was formed after the austenitizing and quenching treatment process used to enhance the impact toughness. Moreover, phase transformation occurred, which improved the hardness and wear resistance. In our published paper, Q&P heat treatment was adopted to obtain retained austenite, and wear resistance was enhanced because of phase transformation from retained austenite with high toughness to martensite with high hardness [28]. However, the relationship between carbon-partitioning parameters and microstructure and between microstructure and mechanical properties (i.e., microhardness, impact toughness, and wear resistance) were unclear. Carbon partitioning is considered as one of the most important treatment methods that can stabilize austenite at room temperature [29−30]. Therefore, carbon-partitioning treatment is conducted to adjust the content of retained austenite, as well as the shape, size, and content of VC in the matrix.

In this study, carbon-partitioning treatment with different holding temperatures and holding times was conducted to stabilize austenite. The effects of holding temperature and holding time on the microstructure, mechanical properties, and wear resistance of *in situ* VCFC were investigated systematically. Then, the wear mechanism was determined through the analysis of the quantitative correlation between weight loss, wear depth, wear width, and wear time. Meanwhile, microstructural characterization and composition analysis were conducted to verify the effect of carbon-partitioning treatment on the wear resistance.

2. Experimental

An *in situ* VCFC with the chemical composition (wt%) of 8.1V–3.0Mn–2.8C–2.5Cr–1.5Mo–1.5Si–(bal.)Fe was used in this study. The investigated composite (VCFC) was prepared through induction melting and casting. The preparation procedure was described in detail in our previous work [28]. The heat treatment process was performed using the muffle and salt bath furnaces. Specimens with a cube size of 20 mm × 55 mm × 10 mm were cut from the cast ingot. First, all specimens were austenitized at 1000°C for 30 min and rapidly quenched in the salt bath furnace (55wt% KNO_3 + 45wt% $NaNO_2$, the melting point was 130°C and the service temperature ranged between 150 and 500°C) at 300°C for 5 min. Then, all specimens underwent carbon-partitioning treatment at holding temperatures of 280, 320, 360, and 400°C and holding times of 5, 15, 30, 45, and 80 min. Finally, all specimens were cooled in water.

The hardness, impact toughness, and wear resistance of the VCFC were measured. After heat treatment, samples for the impact toughness, hardness, and wear tests were cut, with the sizes of 55 mm × 10 mm × 10 mm, 10 mm × 10 mm × 10 mm, and 31 mm × 7 mm × 6 mm, respectively. First, the hardness test was conducted on a Zwick Roell Indentec Vickers tester (ZHV1-AFC, Germany) and the load was set to 9.8 N with the holding time of 15 s. The average value of hardness was calculated with five points and converted into Rockwell hardness. The effects of different holding temperatures and holding times on hardness were also evaluated. Second, impact tests were performed to determine impact toughness of the VCFC (under different holding temperatures and times) using a JBW-300B pendulum-type impact testing machine with an impact energy of 150 J. Each group (each holding temperature or time) included three specimens which were prepared without a notch. The average value was considered the final result. Third, a block-on-cylinder-type wear test machine (M2000, China) was used to measure the wear resistance of the samples with a load of 200 N and rotational speed of 400 r/min. The schematic diagram of the wear resistance test is shown in Fig. 1. The relative size of the counterpart and samples were also presented. The counterpart of the cylinder was YG8 hard alloy, whose hardness is HRA 89. The weight loss, wear width, and wear depth of the wear tracks were measured using an analytical balance, a reading microscope (JC10, China), and an ultra-deep field

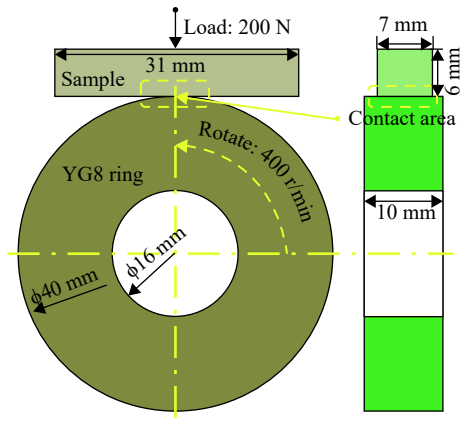

Fig. 1. Schematic diagram of the wear resistance test.

3D microscope (VHX5000, Japan), respectively. The quantitative correlation between weight loss, wear depth, wear width, and wear time was analyzed, and the effects of different carbon-partitioning parameters on the wear resistance of materials were evaluated.

To characterize the microstructure, the samples were etched with a 4.0vol% nitric acid alcohol solution for 30 s in the matrix. Meanwhile, the shape, size, and distribution of VC were characterized by a scanning electron microscope (SEM; TESCAN, MIRA 3 LMH/LMU, Czech Republic) operated at 20 kV. In addition, the chemical composition of the samples was determined using high-energy X-ray diffraction (XRD; Bruker, D8 Discover with TXS, Germany) with Cu K_α radiation source at a rate of 0.5°/s in the 2θ interval ranging from 20° to 100°. The fracture morphology of the specimens after the impact test was also characterized by SEM. Moreover, the morphologies and chemical compositions of the wear tracks were observed by SEM and energy-dispersive spectroscopy (EDS, Oxford, X-Max20, England) to determine the wear mechanism.

3. Results

3.1. Microstructure and composition analysis

Fig. 2 depicts the effects of holding temperatures on the microstructure of as-treated specimens. Notably, the holding temperature has an obvious influence on the shape, size, and distribution of VC. With the increase of holding temperature, large carbide aggregations gradually decrease. A thick flower-like large network structure can be detected at the holding temperatures of 280 and 320°C. However, the thick flower-like large network structure evolves into a slender chrysanthemum-like structure when the holding temperature is 360°C. Moreover, carbide particles are nearly evenly distributed under the holding temperature of 400°C.

To determine the phase structure of the carbide aggregations, XRD analysis was conducted. Fig. 3 shows the XRD test curves at different holding temperatures. Notably, the aggregations are mainly VC and the holding temperature has an obvious influence on the intensity of peaks, particularly within 36.5° to 38°, 41.5° to 47°, 57.5°, 90°, and 95°. Spe-

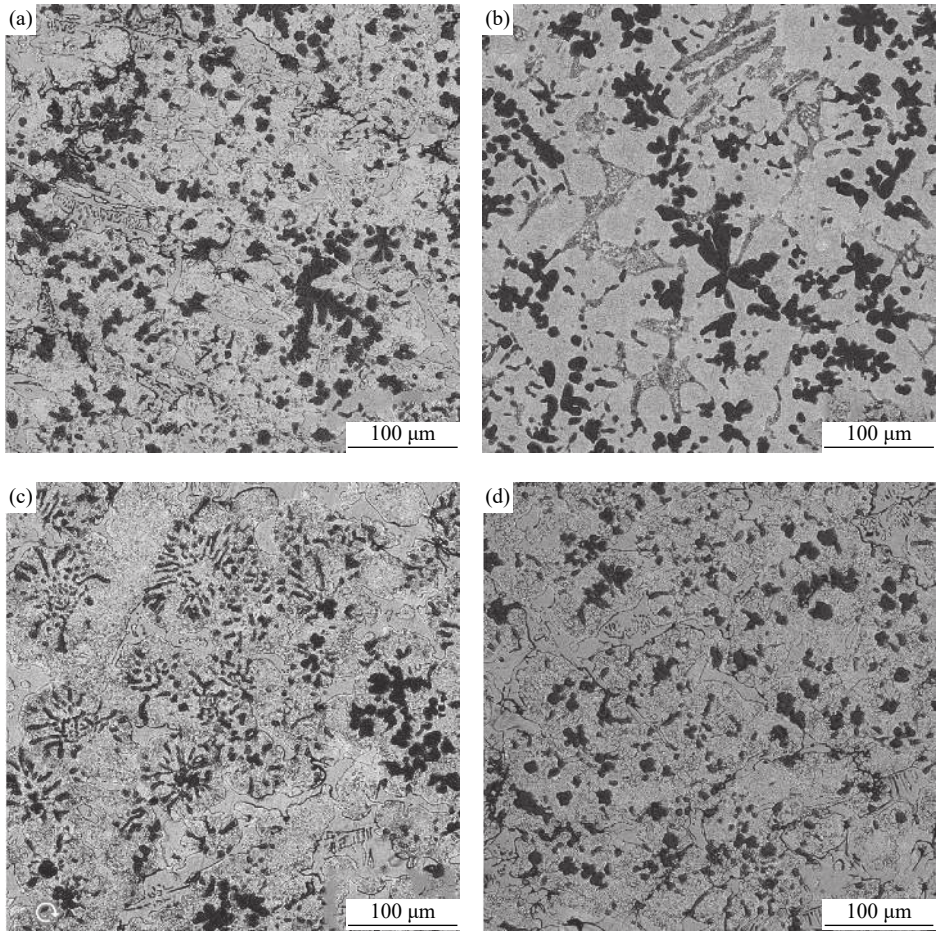

Fig. 2. Microstructures of the VCFC under a constant holding time of 30 min and different holding temperatures: (a) 280°C; (b) 320°C; (c) 360°C; (d) 400°C.

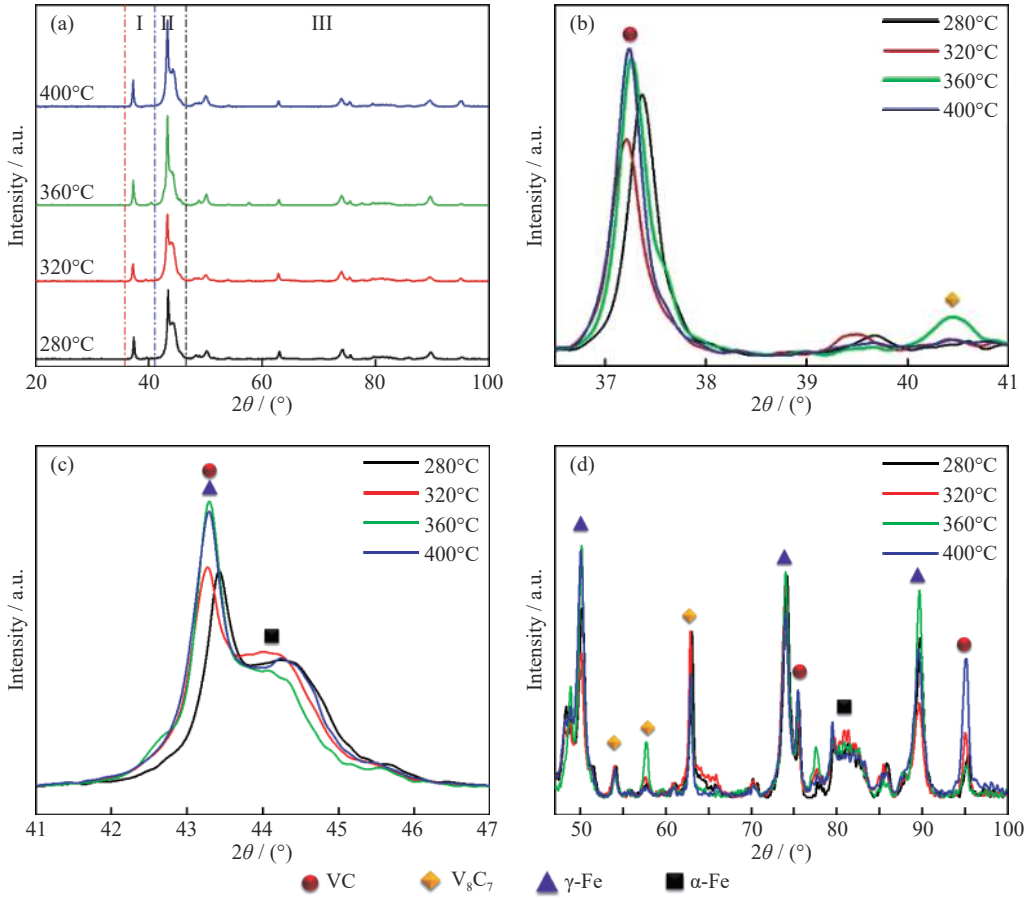

Fig. 3. XRD phase structure analyses in 2θ ranging from 20° to 100° (a), within 36.5° to 41° (b), within 41° to 47° (c), and within 47° to 100° (d), showing the effect of holding temperature on the phase structure of the VCFC.

cifically, the strongest peak within 36.5° to 38° is identified as VC-type carbide at the holding temperature of 400°C. However, this peak offsets a small angle due to retained stress when the holding temperature is 280°C. Meanwhile, a small offset of two Fe peaks existed within 41.5° to 47°. γ-Fe and α-Fe are distributed within 43.25° and 44.25°, respectively. When the holding temperature is 360°C, the γ-Fe peak at 43.25° is larger than that under other temperatures. In addition, the γ-Fe peak at 57.5° and 90° under the carbon-partitioning temperature of 360°C is also larger than that under other temperatures. However, the α-Fe peak at 95° is the smallest.

To further understand the effect of carbon-partitioning treatments on the mechanical properties of the investigated composite, the microstructure and composition of two typical carbon-partitioning treatments were characterized/analyzed by SEM and EDS. Fig. 4 illustrates the microstructure and composition under the holding time of 30 min and the holding temperature of 320°C. Fig. 4(a) shows that four different textures existed in the matrix. Strip VC of submicron scale was detected in region I under magnification. EDS analysis showed that the atomic ratio of vanadium and carbon in region I is 8:7. This finding indicates that the strip VC in region I is V_8C_7 (Fig. 4(b)). Thus, the coarse or globular particles are determined to be VC-type carbide at the vanadium-to-carbon atomic ratio of 1:1 (Fig. 4(c)). Uniquely, the irregular and white compound observed in Fig. 4(d) was determined to be M_3C-type carbide and reported in the literature [30]. In terms of matrix structure, α-Fe and γ-Fe coexist in the matrix [31], and the content of α-Fe is higher than that of γ-Fe, as shown in Figs. 4(c) and 4(d). In addition, the microstructure and composition under the holding time of 30 min and the holding temperature of 360°C are presented in Fig. 5. Other precipitates were more obvious in the matrix structure than in the V_8C_7/VC-type and M_3C-type carbides. Nanoscale rod-like, plate-like, and nanoparticle compounds were detected using high-energy SEM. The nanoscale rod-like compound is distributed around V_8C_7, and the main element is the Fe–C compound accompanied by a small number of Si particles. The main component of the plate-like compound is Fe–Cr–C. This plate-like compound can be $(Fe,Cr)_3C$-type carbide, as reported in the literature [32–33].

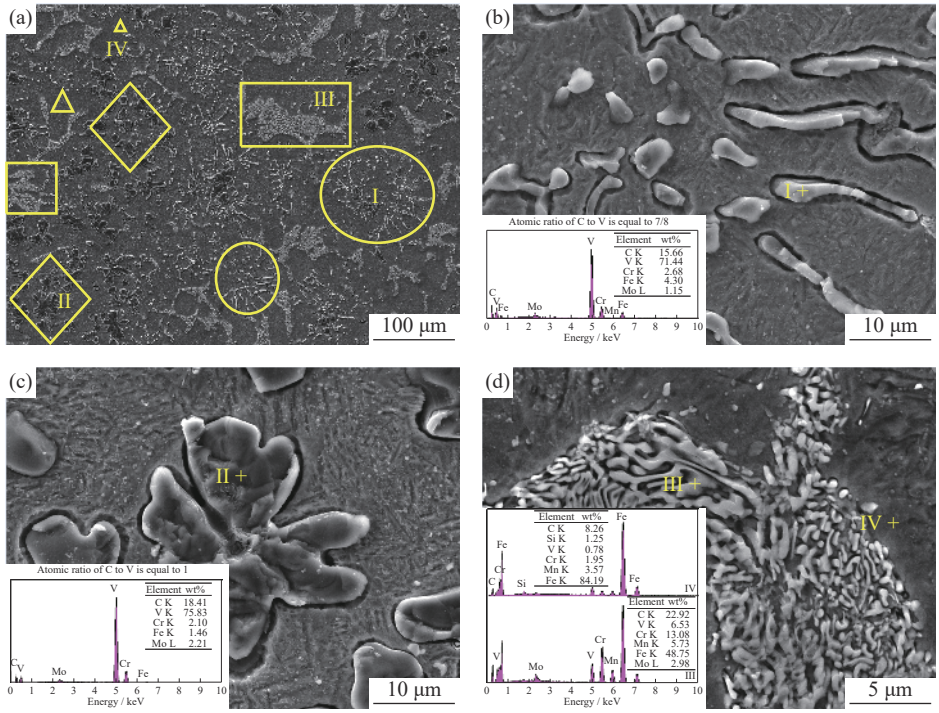

Fig. 4. Microstructure and composition of the VCFC under the carbon-partitioning time of 30 min and the carbon-partitioning temperature of 320°C: (a) sketch maps of different morphologies; (b) lath-like V_8C_7; (c) granulated VC; (d) Fe-matrix.

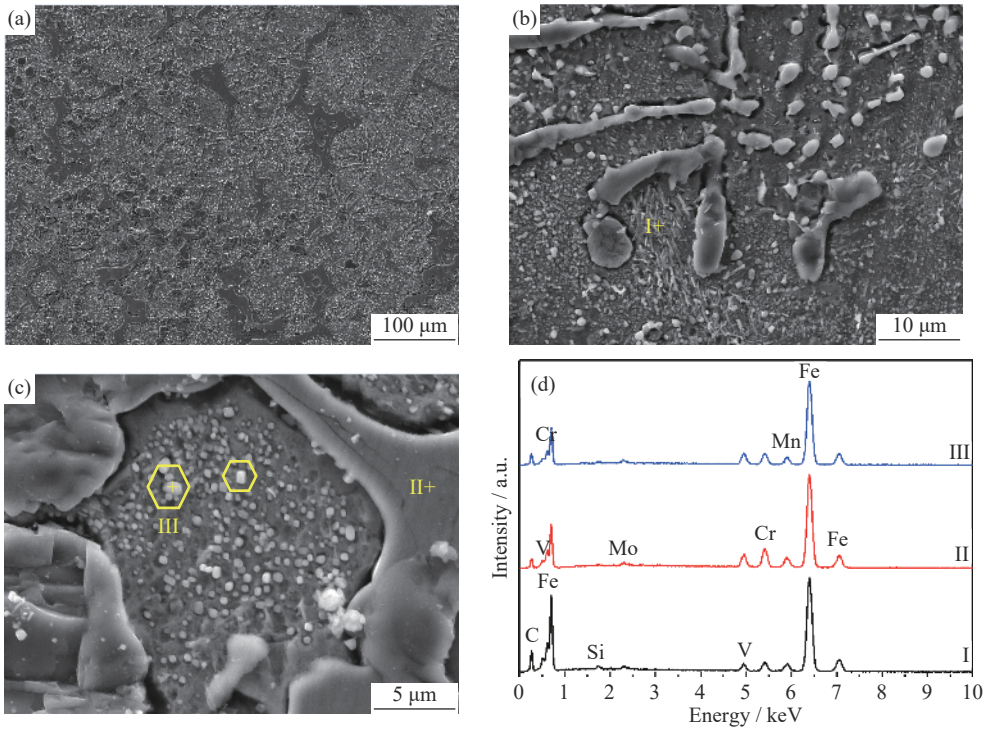

Fig. 5. Microstructure and composition of the VCFC under the holding time of 30 min and the holding temperature of 360°C: (a) sketch maps of different morphologies; (b) nanoscale rod-like compound; (c) plate-like and nanoparticle compounds; (d) EDS composition analysis of regions I, II, and III in (b) and (c) under magnification.

However, the nanoparticle compound can be regarded as supersaturated α-Fe (martensite). Meanwhile, γ-Fe exists in the matrix.

In addition, the effect of holding time on the microstruc-

ture of as-treated specimens is shown in Fig. 6. Notably, the shape, size, and distribution of VC exhibit a significant difference between different holding times. Large aggregations and uneven distribution of VC can be observed under the holding time of 5 min. As the holding time increases to 15 min, VC particles accompanied by a small number of chrysanthemum-like V_8C_7 structures are diffusely distributed in the matrix. However, the proportion of chrysanthemum-like V_8C_7 structures under the holding time of 30 min is larger than that under other holding times. With the sustained increase of holding time, the slender chrysanthemum-like structure finally evolves into a large dendritic structure. In addition, the composition of as-treated specimens changes with the holding time, as shown in Fig. 7. Notably, the γ-Fe peak of the 30 min treated sample reaches its maximum among different holding times. Meanwhile, the minimum α-Fe peak is detected at 44.25° compared with the samples under other treatment times, as shown in Figs. 7(b) and 7(c). In addition, the γ-Fe peak at approximately 50.5°, 73.8°, and 89.2° under the carbon-partitioning time of 30 min is larger than that under other carbon-partitioning times.

3.2. Microhardness and impact toughness

Fig. 8 shows the contour plots of the measured hardness under different holding temperatures and holding times. According to the experimental data of hardness tests, the average hardness of the 280°C treated sample has a minimum value, whereas that of the 360°C treated sample reaches a maximum value. In contrast to the range of the four groups under different holding temperatures, the maximum range was detected in the 320°C treated sample. The hardness values under different holding times of 5, 15, 30, 45, and 80 min were HRC 48.87, 46.87, 50.4, 48.67, and 49.17, respectively. Fig. 8(b) presents the contour plots of the measured impact toughness under different holding temperatures and holding times. Moreover, the measured values of impact toughness under different carbon-partitioning treatments are generally two to three times larger than that of as-cast (AC) specimen. Interestingly, the impact toughness is not always in inverse ratio to the hardness. The range of the 320°C treated samples is only inferior to the range of the 400°C treated samples. Moreover, the values of the 320°C treated samples with the carbon-partitioning time of 5, 15, 30, 45, and 80 min are 7.42, 7.2, 5.99, 7.2, and 7.32 J/cm^2, respectively.

Fig. 9 shows the fracture morphologies under different holding temperatures. The experimental results indicated that typical brittle fracture can be observed under the holding temperature of 320°C, which can be attributed to the coarse

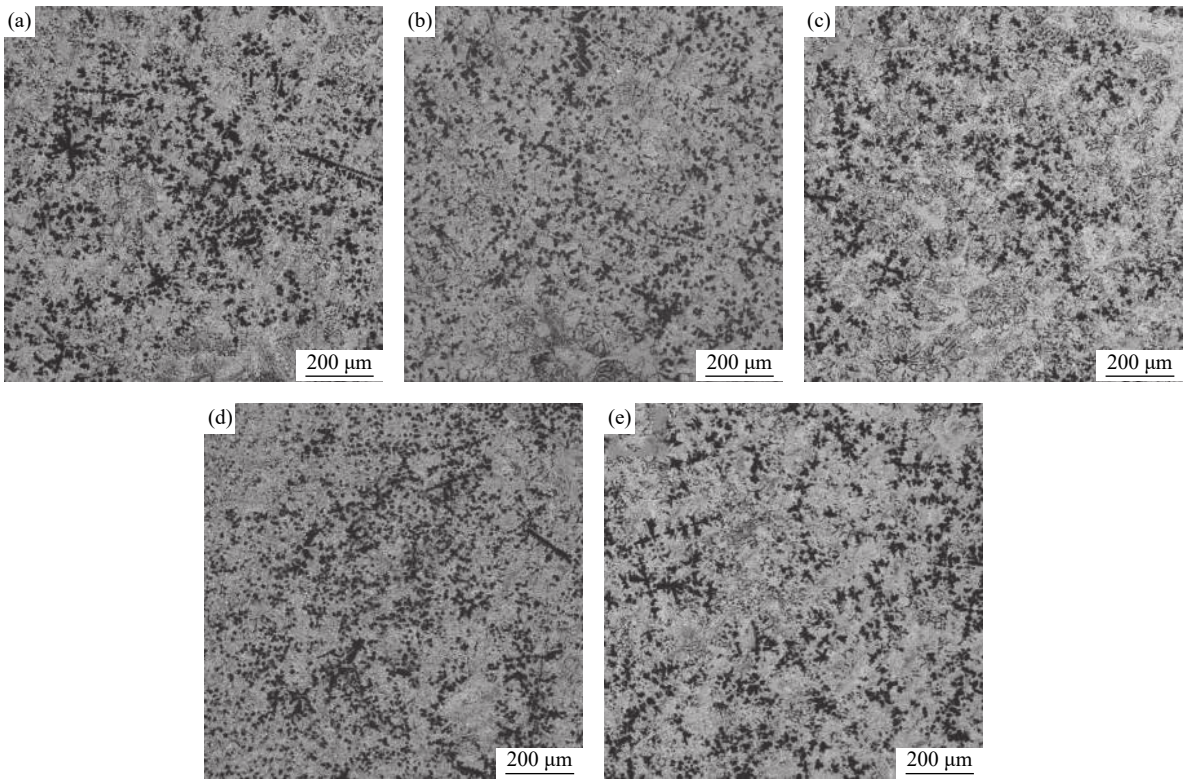

Fig. 6. Microstructures of the VCFC under a constant holding temperature of 360°C and different carbon-partitioning times: (a) 5 min; (b) 15 min; (c) 30 min; (d) 45 min; (e) 80 min.

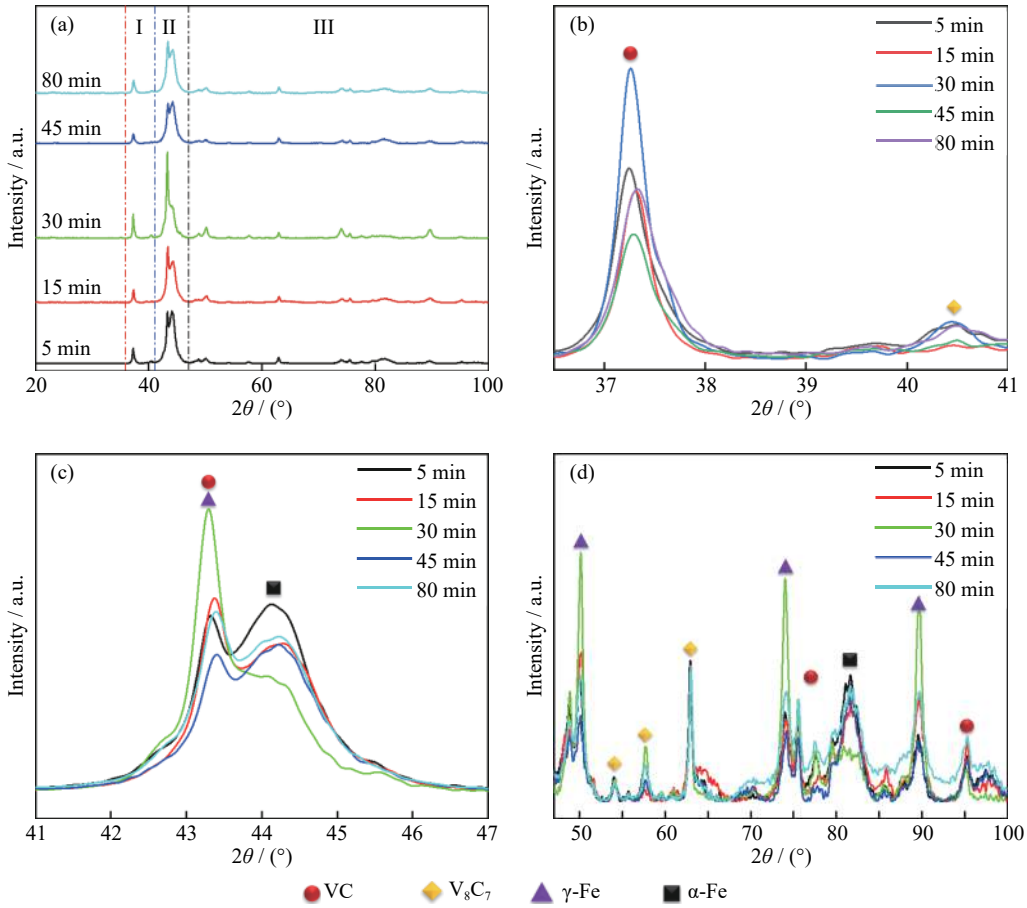

Fig. 7. XRD phase structure analyses in 2θ ranging from 20° to 100° (a), within 36.5° to 41° (b), within 41° to 47° (c), and 47° to 100° (d), showing holding times on the phase structure of the VCFC.

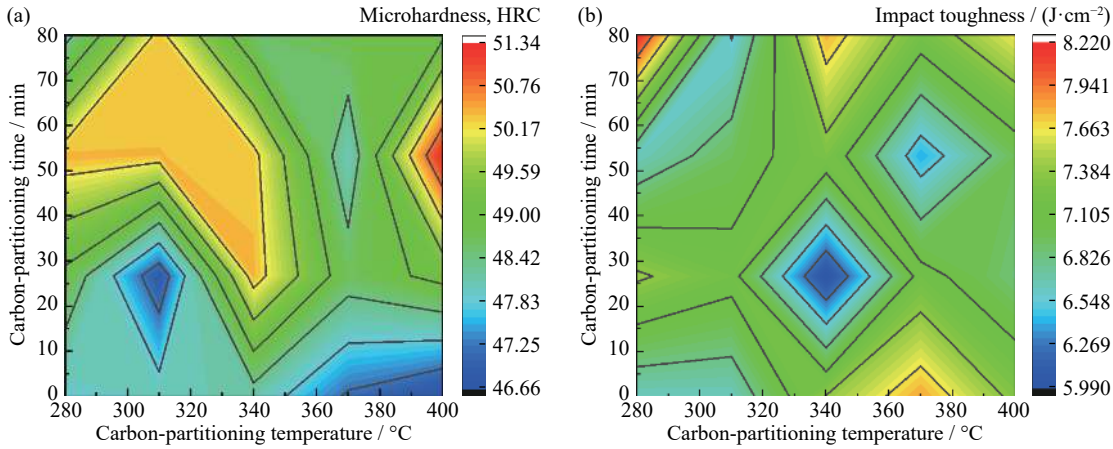

Fig. 8. Hardness (a) and impact toughness (b) of the VCFC under different carbon-partitioning treatments.

and brittle dendritic VC distributed uniformly in the matrix. Thus, the impact toughness under the holding temperature of 320°C (5.99 J/cm^2) is lower than that under other holding temperatures. Generally, dimples are an important parameter in the evaluation of impact toughness. Fig. 9 shows that dimples under the holding temperatures of 360 and 400°C are deeper than that under the holding temperature of 320°C. The dimple area under the holding temperature of 280°C is larger than that under the holding temperature of 320°C.

3.3. Wear resistance

Figs. 10(a) and 10(b) show the weight loss of the AC and

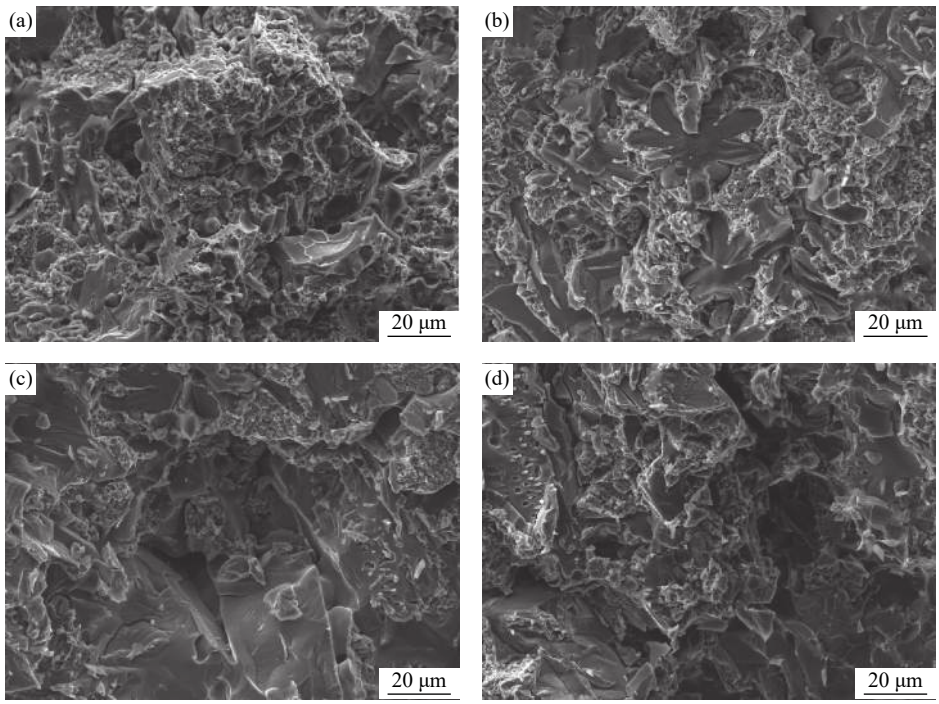

Fig. 9. Fracture morphologies of the VCFC under the carbon-partitioning time of 30 min and the carbon-partitioning temperatures of (a) 280°C, (b) 320°C, (c) 360°C, and (d) 400°C.

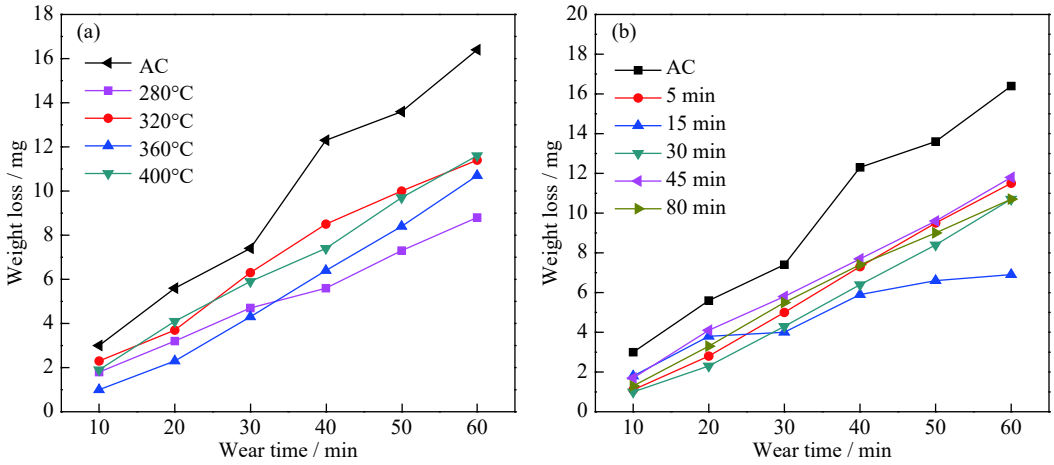

Fig. 10. Weight loss evolution of the VCFC under different holding temperatures (a) and different holding times (b).

as-treated specimens under different holding temperatures and holding times. Notably, the weight loss gradually increases with the increase of the wear time. The weight loss of the as-treated specimens is smaller than that of the AC specimen. In Fig. 10(a), the order of weight loss is $\Delta m_{AC} > \Delta m_{400} > \Delta m_{320} > \Delta m_{360} > \Delta m_{280}$ (Δm expressed the weight loss of specimens within a wear time of 60 min. AC, 280, 320, 360, and 400 represented as-cast, 280, 320, 360, and 400°C treated specimen, respectively) when the wear time is 60 min. The weight loss of the as-treated sample under the holding temperature of 280°C is approximately 9 mg, whereas that of the AC sample is greater than 16 mg. In Fig. 10(b), the wear rate gradually decreases with the increase of wear time under the holding time of 15 min. The weight loss is only 6.9 mg when the wear time reaches 60 min. The results of weight loss may be inadequate to evaluate the effect of carbon-partitioning treatment on the wear resistance of the investigated composite. Therefore, the microstructure and composition of wear tracks were measured using SEM and EDS, as shown in Fig. 11. Notably, tungsten was detected in the wear tracks and it is considered as the alloying element of YG8 hard alloy counterpart. Therefore, the depth and width of the wear

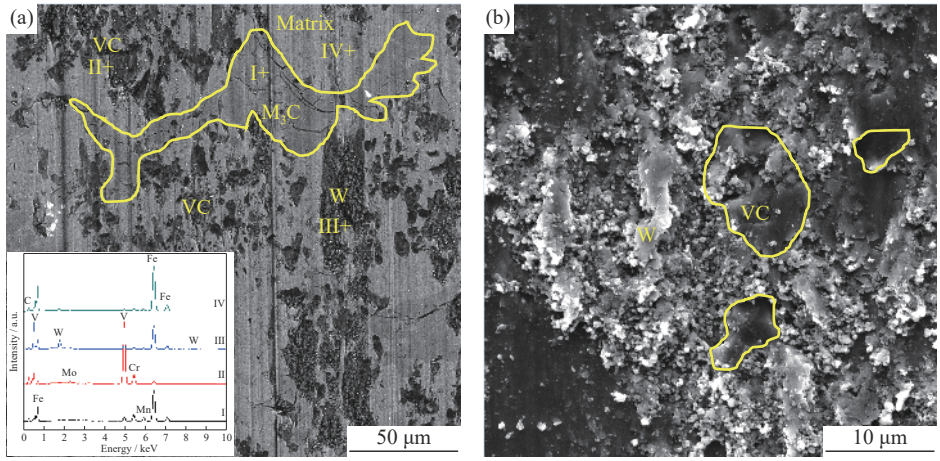

Fig. 11. Morphology characterization and composition analysis of the VCFC's wear tracks with backscatter diffraction image (a) and secondary electron image (b).

tracks should be measured to comprehensively evaluate the wear resistance under different carbon-partitioning treatments.

In addition, the effects of holding temperature and holding time on wear width are presented in Fig. 12. With the increase of wear time, the wear width increases sharply and then slowly. The wear width of the AC specimen is small within 20 min, but its value with a wear time of 60 min is bigger than that under carbon-partitioning treatment. In addition, the wear width reaches its minimum value under the holding temperature of 280°C and holding time of 15 min. By contrast, Fig. 13 illustrates the effect of holding temperatures and holding times on the wear depth. The wear depth under the holding temperatures of 280°C and 360°C is smaller than that under other holding temperatures. However, Fig. 13(b) shows that, with the increase of the holding time, the wear depth initially decreases and subsequently increases. The minimum value was observed under the holding time of 30 min.

4. Analysis and discussion

VC was *in situ* formed from vanadium and carbon in the process of the solidification. Moreover, the shape, size, and distribution of VC were changed through heat treatment, such as austenitizing, quenching, and partitioning treatments. Notably, carbon-partitioning treatment has the most important role in stabilizing austenite at room temperature. The corresponding results were characterized in Figs. 2 to 7. Given the existence of retained austenite, which has excellent toughness, the microhardness decreased, but impact toughness substantially increased.

For the tribological behavior of VCFC, when the microhardness is less than HRC 58, the wear resistance mainly depends on the microhardness of the material. By contrast, when the microhardness is greater than HRC 58, the wear resistance is mainly governed by the shape, size, and distribution of VCp [10,34]. In this study, the microhardness decreased after carbon-partitioning treatment, but the wear res-

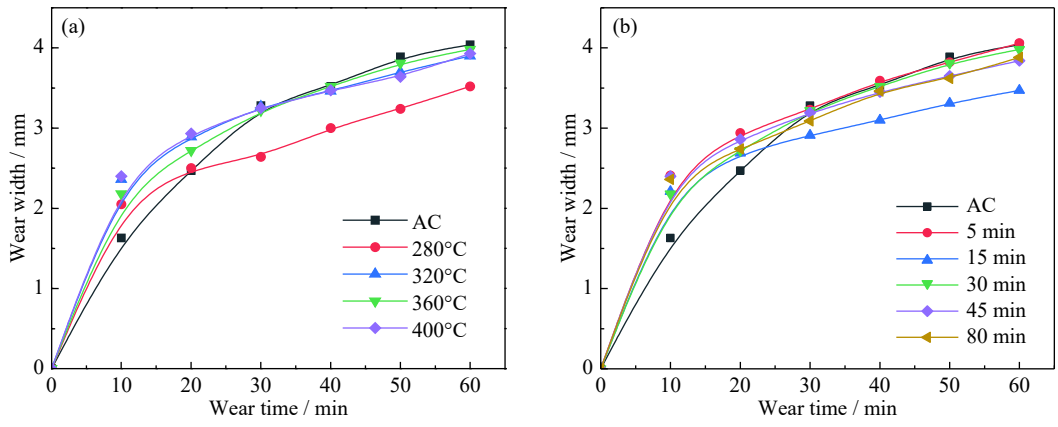

Fig. 12. Wear width evolution of the VCFC under different holding temperatures (a) and different holding times (b).

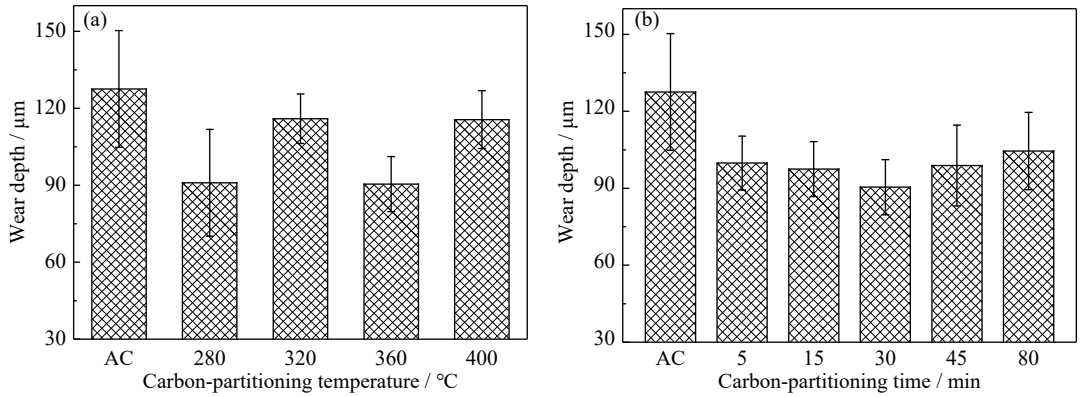

Fig. 13. Wear depth of the VCFC under different holding temperatures (a) and different holding times (b).

istance considerably increased. The main reasons for the improvement of wear resistance were attributed to the following factors: On one hand, the size, shape, and distribution of VC changed in the process of heat treatment. VC has excellent hardness and can resist the serious wear of the counterpart. On the other hand, a certain amount of retained austenite existed steadily at room temperature. Thus, brittle fracture and cracks did not occur. Meanwhile, on the basis of the performance testing results and microstructural characterization, the wear mechanism of the investigated composite is revealed in Fig. 14.

Under the running-in stage of friction, serious wear occurred because of the low hardness and the exposure of few VCp on the surface. After a while, more VCp were exposed on the surface and resisted the wear of the counterpart. Therefore, the wear rate slowed down and serious wear of the counterpart increased, as shown in Fig. 11. In addition, lattice distortion of the retained austenite could occur under a

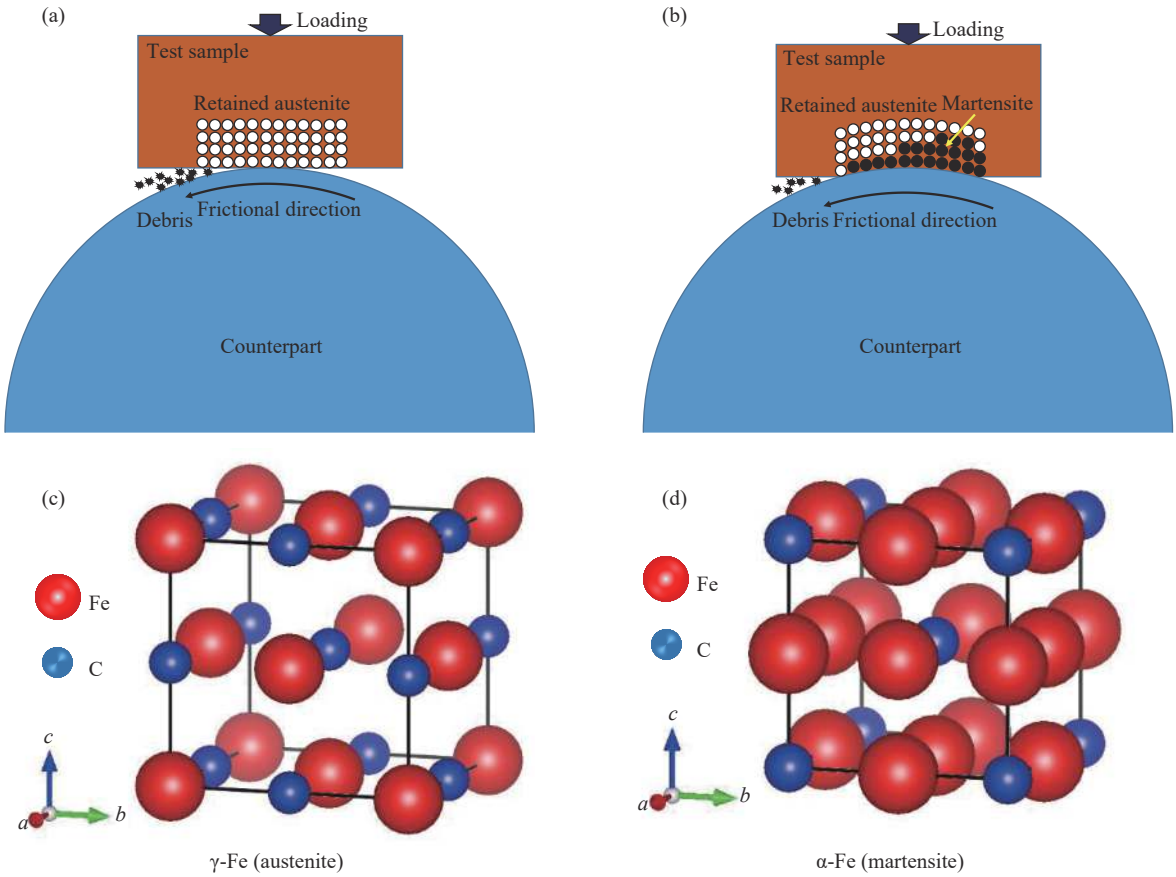

Fig. 14. Wear mechanism of the VCFC: (a) the early stage of friction; (b) the steady stage of friction; (c) the crystal structure of γ-Fe; (d) the crystal structure of α-Fe.

certain load and crystal structures were transferred from face-centered cubic (fcc, retained austenite) to body-centered cubic (bcc, martensite), as shown in Figs. 14(c) and 14(d). Afterward, work hardening of the surface occurred and the overall hardness was improved, thus resulting in the improvement of the wear resistance [35−37].

5. Conclusions

An *in situ* VCFC is heat-treated under different carbon-partitioning conditions. The microstructure, microhardness, toughness, and wear resistance of the as-treated specimens are evaluated. The main conclusions are as follows.

(1) Carbon-partitioning treatment can stabilize the retained austenite at room temperature. The shape, size, and distribution of VC govern the microhardness and impact toughness of the investigated composite.

(2) Given the high microhardness value, the wear resistance of the AC specimens is better than that of the as-treated specimens in the early stage of wear resistance test. However, in the later stage, the as-treated specimen has a low wear rate because of the transformation of retained austenite to martensite.

Acknowledgements

This work was financially supported by the China Postdoctoral Foundation (No. 2019M650339), Guangdong Basic and Applied Basic Research Foundation (No. 2019A1515011858), Hunan Provincial Natural Science Foundation, China (No. 2019JJ50807), the State Key Laboratory of High Performance Complex Manufacturing, China (No. ZZYJKT2017-01), the DGUT Innovation Center of Robotics and Intelligent Equipment of China (No. KCYCXPT2017006), and the Key Laboratory of Robotics and Intelligent Equipment of Guangdong Regular Institutions of Higher Education, China (No. 2017KSYS009).

References

[1] R.R. Moskalyk and M.A. Alfantazi, Processing of vanadium: a review, *Miner. Eng.*, 16(2003), No. 9, p. 793.

[2] M. Radulovic, M. Fiset, K. Peev, and M. Tomovic, The influence of vanadium on fracture toughness and abrasion resistance in high chromium white cast irons, *J. Mater. Sci.*, 29(1994), No. 19, p. 5085.

[3] L.S. Zhong, M. Hojamberdiev, F.X. Ye, W. Hong, and Y.H. Xu, Fabrication and microstructure of *in situ* vanadium carbide ceramic particulates-reinforced iron matrix composites, *Ceram. Int.*, 39(2013), No. 1, p. 731.

[4] L. He, Y. Liu, B.H. Li, H. Cao, and J. Li, Reaction synthesis of *in situ* vanadium carbide particulates-reinforced iron matrix composites by spark plasma sintering, *J. Mater. Sci.*, 45(2010), No. 9, p. 2538.

[5] L.S. Zhong, F.X. Ye, Y.H. Xu, and J.S. Li, Microstructure and abrasive wear characteristics of *in situ* vanadium carbide particulate-reinforced iron matrix composites, *Mater. Des.*, 54(2014), p. 564.

[6] Y.S. Wang, Y.C. Ding, J. Wang, F.J. Cheng, and J.G. Shi, *In situ* production of vanadium carbide particulates reinforced iron matrix surface composite by cast-sintering, *Mater. Des.*, 28(2007), No. 7, p. 2202.

[7] M. Kawalec and E. Olejnik, Abrasive wear resistance of cast iron with precipitates of spheroidal VC carbides, *Arch. Foundry Eng.*, 12(2012), No. 2, p. 221.

[8] W.M. Zhao, Z.X. Liu, Z.L. Ju, B. Liao, and X.G. Chen, Effects of vanadium and rare-earth on carbides and properties of high chromium cast iron, *Mater. Sci. Forum*, 575-578(2008), p. 1414.

[9] F.X. Ye, M. Hojamberdiev, Y.H. Xu, L.S. Zhong, H.H. Yan, and Z. Chen, $(Fe,Cr)_7C_3$-Fe surface gradient composite: Microstructure, microhardness, and wear resistance, *Mater. Chem. Phys.*, 147(2014), No. 3, p. 823.

[10] S.Z. Wei, J.H. Zhu, and L.J. Xu, Research on wear resistance of high speed steel with high vanadium content, *Mater. Sci. Eng. A*, 404(2005), No. 1-2, p. 138.

[11] S.Z. Wei, J.H. Zhu, and L.J. Xu, Effects of vanadium and carbon on microstructures and abrasive wear resistance of high speed steel, *Tribol. Int.*, 39(2006), No. 7, p. 641.

[12] S.Z. Wei, J.H. Zhu, L.J. Xu, and R. Long, Effects of carbon on microstructures and properties of high vanadium high-speed steel, *Mater. Des.*, 27(2006), No. 1, p. 58.

[13] J.X. Liu, Z.W. Shi, P.J. Ying, S.Z. Guo, W.L. Ji, and R. Long, Effect of carbon on frictional wear behaviours of high vanadium high speed steel under dry sliding condition, *Mater. Sci. Forum*, 654-656(2010), p. 370.

[14] L.J. Xu, J.D. Xing, S.Z. Wei, Y.Z. Zhang, and R. Long, Study on relative wear resistance and wear stability of high-speed steel with high vanadium content, *Wear*, 262(2007), No. 3-4, p. 253.

[15] M. Krüger, High temperature compression strength and oxidation of a V−9Si−13B alloy, *Scripta Mater.*, 121(2016), p. 75.

[16] P.H. Chen, Z.L. Liu, R.Q. Li, and X.Q. Li, The effect of manganese additions on the high temperature oxidation behaviour of the high-vanadium cast iron, *J. Alloys Compd.*, 767(2018), p. 181.

[17] P.H. Chen, R.Q. Li, R.P. Jiang, S.S. Zeng, Y. Zhang, and X.Q. Li, High-temperature oxidation resistance of VCps-reinforced Fe-matrix composites using an *in-situ* reaction, *AIP Adv.*, 9(2019), No. 1, p. 015319.

[18] V.F. Zackay, M.D. Bhandarkar, and E.R. Parker, The role of deformation-induced phase transformations in the plasticity of some iron-base alloys, [In] J.J. Burke and V. Weiss, eds., *Advances in Deformation Processing*, Boston, MA, 1978, p. 351.

[19] L. Skálová, R. Divišová, and D. Jandová, Thermo-mechan-

ical processing of low-alloy TRIP-steel, *J. Mater. Process. Technol.*, 175(2006), No. 1-3, p. 387.

[20] J. Speer, D.K. Matlock, B.C. de Cooman, and J.G. Schroth, Carbon partitioning into austenite after martensite transformation, *Acta Mater.*, 51(2003), No. 9, p. 2611.

[21] J.G. Speer, E. De Moor, K.O. Findley, D.K. Matlock, B.C. de Cooman, and D.V. Edmonds, Analysis of microstructure evolution in quenching and partitioning automotive sheet steel, *Metall. Mater. Trans. A*, 42(2011), No. 12, p. 3591.

[22] V.F. Zackay and T.H. Hazlett, Some plastic properties of nickel alloys, *Acta Metall.*, 1(1953), No. 6, p. 624.

[23] P.J. Gibbs, E. de Moor, M.J. Merwin, B. Clausen, J.G. Speer, and D.K. Matlock, Austenite stability effects on tensile behavior of manganese-enriched-austenite transformation-induced plasticity steel, *Metall. Mater. Trans. A*, 42(2011), No. 12, p. 3691.

[24] M. Mansourinejad and M. Ketabchi, Influence of strain state on the kinetics of martensitic transformation induced plasticity (TRIP) in AISI 304 stainless steel, *Steel Res. Int.*, 89(2018), No. 3, p. 1700359.

[25] A.J. Clarke, J.G. Speer, M.K. Miller, R.E. Hackenberg, D.V. Edmonds, D.K. Matlock, F.C. Rizzo, K.D. Clarke, and E. De Moor, Carbon partitioning to austenite from martensite or bainite during the quench and partition (Q&P) process: A critical assessment, *Acta Mater.*, 56(2008), No. 1, p. 16.

[26] J.G. Speer, D.V. Edmonds, F.C. Rizzo, and D.K. Matlock, Partitioning of carbon from supersaturated plates of ferrite, with application to steel processing and fundamentals of the bainite transformation, *Curr. Opin. Solid State Mater. Sci.*, 8(2004), No. 3-4, p. 219.

[27] Z.C. Li, H. Ding, R.D.K. Misra, Z.H. Cai, and H.X. Li, Microstructural evolution and deformation behavior in the Fe−(6, 8.5)Mn−3Al−0.2C TRIP steels, *Mater. Sci. Eng. A*, 672(2016), p. 161.

[28] P.H. Chen, Y.B. Li, R.Q. Li, R.P. Jiang, S.S. Zeng, and X.Q. Li, Microstructure, mechanical properties, and wear resistance of VCp-reinforced Fe-matrix composites treated by Q&P process, *Int. J. Miner. Metall. Mater.*, 25(2018), No. 9, p. 1060.

[29] E. De Moor, S. Lacroix, A.J. Clarke, J. Penning, and J.G. Speer, Effect of retained austenite stabilized via quench and partitioning on the strain hardening of martensitic steels, *Metall. Mater. Trans. A*, 39(2008), p. 2586.

[30] X.C. Xiong, B. Chen, M.X. Huang, J.F. Wang, and L. Wang, The effect of morphology on the stability of retained austenite in a quenched and partitioned steel, *Scripta Mater.*, 68(2013), No. 5, p. 321.

[31] L.J. Xu, S.Z. Wei, J.D. Xing, and R. Long, Effects of carbon content and sliding ratio on wear behavior of high-vanadium high-speed steel (HVHSS) under high-stress rolling-sliding contact, *Tribol. Int.*, 70(2014), p. 34.

[32] V.G. Efremenko, K. Shimizu, A.P. Cheiliakh, T.V. Kozarevskaya, K. Kusumoto, and K. Yamamoto, Effect of vanadium and chromium on the microstructural features of V−Cr−Mn−Ni spheroidal carbide cast irons, *Int. J. Miner. Metall. Mater.*, 21(2014), No. 11, p. 1096.

[33] L.J. Xu, J.D. Xing, S.Z. Wei, Y.Z. Zhang, and R. Long, Investigation on wear behaviors of high-vanadium high-speed steel compared with high-chromium cast iron under rolling contact condition, *Mater. Sci. Eng. A*, 434(2006), No. 1-2, p. 63.

[34] L.J. Xu, S.Z. Wei, F.N. Xiao, H. Zhou, G.S. Zhang, and J.W. Li, Effects of carbides on abrasive wear properties and failure behaviours of high speed steels with different alloy element content, *Wear*, 376-377(2017), p. 968.

[35] V.G. Efremenko, K. Shimizu, A.P. Cheiliakh, T.V. Pastukhova, Y.G. Chabak, and K.Kusumoto, Abrasive resistance of metastable V−Cr−Mn−Ni spheroidal carbide cast irons using the factorial design method, *Int. J. Miner. Metall. Mater.*, 23(2016), No. 6, p. 645.

[36] V.G. Efremenko, K. Shimizu, T.V. Pastukhova, Y.G. Chabak, K. Kusumoto, and A.V. Efremenko, Effect of bulk heat treatment and plasma surface hardening on the microstructure and erosion wear resistance of complex-alloyed cast irons with spheroidal vanadium carbides, *J. Frict. Wear*, 38(2017), No. 1, p. 58.

[37] V. Efremenko, K. Shimizu, T. Pastukhova, Y. Chabak, M. Brykov, K. Kusumoto, and A. Efremenko, Three-body abrasive wear behaviour of metastable spheroidal carbide cast irons with different chromium contents, *Int. J. Mater. Res.*, 109(2018), No. 2, p. 147.